

---

# The surprising strength of weak classifiers for validating neural posterior estimates

---

Vansh Bansal\*, Tianyu Chen\*

Department of Statistics and Data Sciences  
UT Austin  
{vansh,tianyuchen}@utexas.edu

James G. Scott

Department of Statistics and Data Sciences  
McCombs School of Business  
UT Austin  
james.scott@mcombs.utexas.edu

## Abstract

Neural Posterior Estimation (NPE) has emerged as a powerful approach for amortized Bayesian inference when the true posterior  $p(\theta | y)$  is intractable or difficult to sample. But evaluating the accuracy of neural posterior estimates remains challenging, with existing methods suffering from major limitations. Simulation-Based Calibration (SBC), for example, is widely adopted, but offers rigorous guarantees only for one-dimensional parameters, and performs poorly on larger problems. One appealing and widely used alternative is the classifier two-sample test (C2ST), where a classifier is trained to distinguish samples from the true posterior  $p(\theta | y)$  versus the learned NPE approximation  $q(\theta | y)$ . Yet despite the appealing simplicity of the C2ST, its theoretical and practical reliability depend upon having access to a near-Bayes-optimal classifier—a requirement that is rarely met and, at best, difficult to verify. Thus a major open question is: can a weak classifier still be useful for neural posterior validation? We show that the answer is yes. Building on the work of Hu and Lei [1], we present several key results for a conformal variant of the C2ST, which converts any trained classifier’s scores—even those of weak or over-fitted models—into exact finite-sample p-values. We establish two key theoretical properties of the conformal C2ST: (i) finite-sample Type-I error control, and (ii) non-trivial power that degrades gently in tandem with the error of the trained classifier. The upshot is that even weak, biased, or overfit classifiers can still yield powerful and reliable tests. Empirically, the Conformal C2ST outperforms classical discriminative tests across a wide range of benchmarks. These results reveal the underappreciated strength of weak classifiers for validating neural posterior estimates, establishing the conformal C2ST as a practical, theoretically grounded diagnostic for modern simulation-based inference.

## 1 Introduction

Advances in generative modeling have made Neural Posterior Estimation (NPE) an increasingly popular and practical tool for Bayesian inference in complex scientific models. NPE methods use simulations from the true joint distribution,  $p(\theta, y) = p(\theta)p(y | \theta)$ , to generate training pairs  $(\theta, y)$  that represent the relationship between parameters and observations. A neural network—typically a diffusion model [2, 3, 4, 5], normalizing flow [6], or other deep generative architectures [7, 8]—is then trained on these simulations, fitting a model  $q(\theta | y)$  to approximate the true posterior  $p(\theta | y)$ . This approach enables flexible, amortized inference even when the true posterior is intractable or involves a "black box" likelihood.

---

\*equal contribution

Yet despite the growing use of NPE in scientific workflows, the problem of neural posterior validation—that is, assessing whether the learned posterior  $q$  faithfully approximates the true posterior  $p$ —remains challenging. Several methods have been proposed to address this problem, yet they all suffer from drawbacks. Simulation-based calibration (SBC) [9] is perhaps the most widely used diagnostic for this purpose. But it works only for one-dimensional parameters, and it must therefore be applied independently to each margin of  $q$ . This not only creates a potentially severe multiple-testing problem, but it also means that SBC is insensitive to inaccuracies that affect the joint distribution of all parameters without affecting their one-dimensional marginals. TARP [10], or "tests of accuracy by random points," is one recently proposed method to address this shortcoming of SBC. However, TARP's performance depends strongly on a non-trainable proposal distribution for sampling a "reference"  $\theta$ , and the paper's approach for choosing this distribution implicitly assumes that the sample space  $\mathcal{Y}$  and parameter space  $\Theta$  are identical. This condition typically holds only in fairly simple models (e.g. location families or models with sufficient statistics), making it a serious practical limitation.

On the other hand, the classifier-based two-sample test (C2ST) [11] provides a highly flexible alternative to SBC or TARP. The C2ST reframes the problem of distributional comparison as a classification task. In this approach, a classifier is trained to distinguish between samples drawn from the true joint distribution  $p(\theta, y)$ , versus those drawn from the neural approximation  $q(\theta, y)$ . If the classifier achieves high accuracy, it suggests that the samples from  $p$  and  $q$  are distinguishable, indicating a mismatch between the two distributions. Conversely, poor classification performance implies that the two sets of samples are statistically similar, supporting the validity of the approximation. Yet while C2ST is valid under the null—i.e., it controls type-I error asymptotically—its power depends critically on the quality of the classifier, which has the difficult task of learning a global decision boundary over the product space  $\mathcal{Y} \times \Theta$ . In practice, a trained classifier may be weak due to limited training data, restricted model capacity, poor calibration of output probabilities (e.g. thresholding at 0.5), or simply the inherent challenge of the classification problem. This raises a potential ambiguity in interpretation: if a model  $q$  "passes" the C2ST, that could mean either that  $q = p$ , or that  $q \neq p$  but the classifier is too weak or poorly trained to tell the difference.

**Summary of contributions.** Our paper addresses these limitations by presenting new results on a conformal variant of the classifier two-sample test, termed the **Conformal C2ST**. While our work builds on the recent proposal by [1], who studied weighted conformal prediction for testing under distribution shift, their approach is based on constructing a highly accurate model for the true density ratio between the two distributions. A nearly-Bayes-optimal classifier may approximate this ratio, but this leaves a critical gap: what if the classifier is far from optimal? This question is especially pressing in neural posterior estimation, where classifiers used to run the C2ST are often trained on limited data, prone to overfitting, or too weak to learn a global Bayes-optimal decision boundary. In contrast, our work is both theoretically and empirically motivated by this regime of imperfection. We study what happens when the classifier is suboptimal—whether because it is noisy, weak, or under-trained—and show rigorously that conformal calibration can still produce powerful, robust posterior checks, addressing a major gap in our understanding of C2ST-based approaches.

We first show that conformal calibration effectively decouples type-I error control from the classifier's discriminative accuracy. More importantly, we also prove that conformal  $p$ -values maintain meaningful power under the alternative (i.e. when  $p \neq q$ ), even when the classifier is weaker or poorly trained. Intuitively, they do so by aggregating weak but informative ranking signals; we formalize this property, which is especially crucial in scenarios where the traditional C2ST struggles, such as high-dimensional posteriors, small-sample regimes, and tasks with low signal-to-noise ratios. We support our theoretical developments with extensive empirical results, which show that the conformal C2ST exhibits state of the art performance for neural posterior evaluation across a wide range of benchmark problems.

**A toy example** Before detailing our results, we briefly focus on a toy example, to illustrate the fundamental advantage of conformal calibration. The setup mimics the NPE setting, where the marginal distribution of  $y$  is preserved under both the true and approximate joint distributions. Specifically, we consider two bivariate normal distributions:  $p(\theta, y)$  is a standard bivariate normal,  $\mathcal{N}(\mathbf{0}, I_2)$ , while  $q(\theta, y)$  is the same distribution with a mean shift of 0.5 in the  $\theta$  coordinate, i.e.,  $\mathcal{N}([0.5, 0]^\top, I_2)$ . The Bayes-optimal classifier for distinguishing between samples from  $p$  and  $q$  is

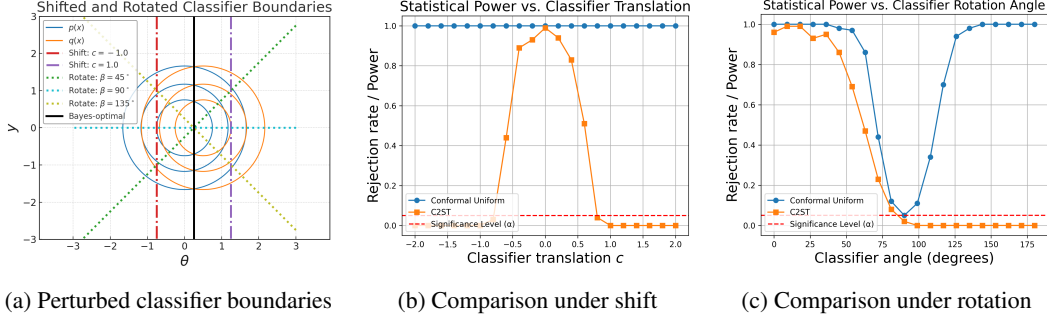


Figure 1: Power of the C2ST and conformal C2ST under shift and rotate perturbations of the optimal decision boundary. The conformal test is much more robust to a weak or misspecified classifier.

a linear decision boundary at  $\theta = 0.25$ , bisecting  $\mathbb{R}^2$  between the two means. Classifier scores are obtained by computing the signed distance from a sample point  $(\theta, y)$  to the decision boundary.

We then degrade the classifier by manipulating the decision boundary in two systematic ways. First is *translation*, where the decision boundary is shifted horizontally by a parameter  $c$ , modifying the decision boundary to  $\theta = 0.25 + c$ . The parameter  $c$  can be positive, shifting the boundary toward  $q$ , or negative, shifting it toward  $p$ . As  $|c|$  increases, the boundary moves further from its optimal position, increasing classification error. As we see in Figure 1b, this rapidly degrades the power of the C2ST for distinguishing  $p$  and  $q$ . Yet the conformal C2ST’s performance remains remarkably stable, showing no degradation in power even for large shifts. This suggests a strong level of robustness to biased or poorly calibrated classifiers. (Although the classifier is trained to distinguish individual draws from  $p$  and  $q$ , the goal of neural posterior testing is to assess whether two *collections* of samples arise from the same distribution, allowing aggregation across multiple draws and yielding greater power than would be expected from single-point classification alone.) The second form of degradation is *rotation*, where the decision boundary is rotated about the midpoint between the means of  $p$  and  $q$ . The boundary under rotation is described by  $(\theta - 0.25) \cos \beta + y \sin \beta = 0$ , where  $\beta$  controls the angle of rotation. A rotation of  $\beta = 0$  corresponds to the optimal linear discriminant, while increasing  $|\beta|$  introduces growing misalignment. Figure 1c shows that the conformal C2ST continues to perform significantly better under quite severe rotations, indicating resilience even when the classifier is badly misaligned. At  $\beta = \pi/2$ , the decision boundary becomes completely orthogonal to the separation axis of the two distributions, rendering the distribution of classifier scores identical under  $p$  and  $q$ . In this extreme case, the conformal C2ST has power 0.05, which is precisely the type-I error rate of the test.

These results illustrate the key advantage of the conformal C2ST: even when the classifier itself becomes progressively poorer or more miscalibrated, its ranking signals nonetheless remain useful.

## 2 Classifier-Based Posterior Testing and Conformal Calibration

### 2.1 Preliminaries

We consider two distributions over joint parameter–observation pairs  $(\theta, y) \in \Theta \times \mathcal{Y}$ : the true posterior  $p(\theta | y)$ , defined via the joint density  $p(\theta, y) = \pi(\theta)p(y | \theta)$ , and an approximate posterior  $q(\theta | y)$ , learned using simulation-based inference (SBI). We are agnostic as to *how*  $q$  was learned; instead, our goal is to assess whether  $q(\theta | y) = p(\theta | y)$  almost surely over  $\Theta \times \mathcal{Y}$ . Assuming a shared marginal  $\pi(y)$ , we define the approximate joint as  $q(\theta, y) := \pi(y)q(\theta | y)$ . Under this assumption, testing equality of posteriors reduces to testing the null hypothesis  $H_0 : p(\theta, y) = q(\theta, y)$  almost surely over  $\Theta \times \mathcal{Y}$ . This naturally frames the problem as a *two-sample test* between the joint distributions  $p(\theta, y)$  and  $q(\theta, y)$ .

In the NPE setting, i.i.d. samples from both  $p$  and  $q$  are readily available. To sample from the true joint  $p$ , we draw  $\theta \sim \pi(\theta)$  and then  $y \sim p(y | \theta)$ . To sample from the approximate joint  $q$ , we use the  $y$  margin only of the true  $p$ , implicitly generating  $y \sim \pi(y)$ , and then we sample  $\theta \sim q(\theta | y)$  from the learned model. For convenience, we write  $x = (\theta, y)$ , and use  $p$  and  $q$  as shorthand for the

true and approximate joint densities over  $x$ . We denote samples as  $\{X_i\}_{i=1}^n \sim p$  and  $\{\tilde{X}_i\}_{i=1}^n \sim q$ . Throughout, we assume that  $p(\theta | y)$  and  $q(\theta | y)$  are absolutely continuous with respect to a common base measure.

**The classifier two-sample test (C2ST).** The C2ST is a widely used approach for detecting differences between two distributions. In the context of posterior validation, suppose we are given two datasets  $\{x_i\}_{i=1}^n \sim p$  and  $\{\tilde{x}_i\}_{i=1}^n \sim q$ . To test the null hypothesis  $H_0 : p = q$ , a classifier is trained to distinguish between the two samples. Specifically, each  $x_i$  is assigned label 1 and each  $\tilde{x}_i$  is assigned label 0, producing a labeled dataset  $\{(z_i, \ell_i)\}_{i=1}^{2n}$ , where  $z_i \in \mathcal{X}$  and  $\ell_i \in \{0, 1\}$ . The combined dataset is randomly split into disjoint training and testing subsets. A classifier  $f : \mathcal{X} \rightarrow [0, 1]$  is trained on the training portion to estimate the conditional probability  $\mathbb{P}[\ell = 1 | z]$ , and evaluated on the test set  $\mathcal{D}_{\text{te}}$ . The C2ST test statistic is the classification accuracy on the test set:

$$\hat{t} := \frac{1}{n_{\text{te}}} \sum_{(z_i, \ell_i) \in \mathcal{D}_{\text{te}}} \mathbb{I}\{\mathbb{I}\{f(z_i) > 1/2\} = \ell_i\},$$

which is shown to have an asymptotic normal distribution in [11]. The null hypothesis  $H_0 : p = q$  is rejected if  $\hat{t}$  is significantly greater than 0.5, indicating that the classifier has learned to distinguish between  $p$  and  $q$ .

While C2ST is easy to implement and effective in many cases, it has two key limitations. First, its power depends heavily on the classifier quality. Poorly trained or underfit classifiers can yield inconclusive results, even when the two distributions differ. Second, its test statistic relies on hard decisions via thresholding at 0.5, discarding potentially useful information about classifier confidence.

## 2.2 The uniform test: conformal calibration of classifier scores

To address these limitations, we adopt a conformal framework that calibrates classifier scores directly, rather than thresholding them. This yields a method we term the *Conformal C2ST*. The core idea is to treat each point as a test case, compute a score for that point (e.g., classifier log-odds), and use a conformal p-value to assess how extreme that score is relative to a calibration sample from the reference distribution ( $p$ ). Each such p-value reflects the plausibility of a single test point from  $q$  under the null. To test whether  $p = q$  globally, we repeat this procedure across many independent draws from  $q$ , aggregating the resulting p-values to assess overall deviation from uniformity. This allows the method to extract and accumulate weak signals for assessing distributional equality, even from underperforming classifiers, by calibrating based on ranks rather than raw accuracy.

Concretely, let  $\{X_1, \dots, X_m\} \sim p$  be a calibration sample and let  $\tilde{X} \sim q$  be a test point. Let  $s : \mathcal{X} \rightarrow \mathbb{R}$  be a deterministic scoring function, which in our case will be the output of a classifier trained to distinguish  $p$  from  $q$ , just like in C2ST. (Below we discuss the specific choice of  $s$ .) Define the nonconformity scores  $S_i = s(X_i)$  for  $i = 1, \dots, m$ , and  $S_{m+1} = s(\tilde{X})$ . The conformal p-value [12, 13] for  $\tilde{X}$  is then given by:

$$U := \frac{1}{m+1} \left( \sum_{i=1}^{m+1} \mathbb{I}\{S_i < S_{m+1}\} + \xi \cdot \sum_{i=1}^{m+1} \mathbb{I}\{S_i = S_{m+1}\} \right), \quad (1)$$

where  $\xi \sim \text{Unif}[0, 1]$  is a tie-breaking random variable. The p-value  $U$  reflects the relative rank of the test point's score among the calibration scores.

## 2.3 Finite-sample validity

A key advantage of this approach is that it inherits the finite-sample validity guarantee from conformal prediction. Under  $H_0$ , the calibration points and the test point are exchangeable, implying the following marginal guarantee.

**Lemma 1** (Uniformity under the null). *Under the null hypothesis  $H_0 : p = q$ , the conformal p-value  $U$  defined in (1) satisfies:*

$$\mathbb{P}(U \leq u | H_0) = u, \quad \forall u \in [0, 1],$$

where the probability is over the random draw of the calibration sample, the test point, and the tie-breaking variable.

This result holds for any deterministic scoring function  $s$  and for any finite calibration size  $m$ , making the conformal C2ST robust to classifier quality and sample size. This result is a standard property of conformal inference; see [12, 13].

**From marginal p-values to a uniformity test.** To turn the marginal validity established in Lemma 1 into a global two-sample test of  $H_0 : p = q$ , we repeat the conformal p-value computation across multiple test points. Specifically, let  $\{\tilde{X}_j\}_{j=1}^{n_q} \sim q$  be independent test samples. For each  $j$ , we draw an independent calibration set  $\mathcal{C}_j = \{X_{j,i}\}_{i=1}^m \sim p$ , and compute the corresponding conformal p-value

$$U_j := \frac{1}{m+1} \left( \sum_{i=1}^{m+1} \mathbb{I} \left\{ s(X_{j,i}) < s(\tilde{X}_j) \right\} + \xi_j \cdot \sum_{i=1}^{m+1} \mathbb{I} \left\{ s(X_{j,i}) = s(\tilde{X}_j) \right\} \right),$$

where  $X_{j,m+1} = \tilde{X}_j$ , and  $\xi_j \sim \text{Uniform}[0, 1]$  are independent tie-breaking variables. Under  $H_0$ , each  $U_j \sim \text{Unif}[0, 1]$ , so we can aggregate the  $\{U_j\}$  to form a global test statistic. We consider the empirical CDF  $\hat{G}(u) = \frac{1}{n_q} \sum_{j=1}^{n_q} \mathbb{I}\{U_j \leq u\}$  and apply the one-sample Kolmogorov–Smirnov (KS) test [14], using

$$T_{\text{KS}} = \sup_{u \in [0,1]} \left| \hat{G}(u) - u \right|.$$

Because  $H_0 : p = q$  implies exchangeability between the calibration and test samples, each  $U_j$  is uniformly distributed, and the KS test (or any similar test) controls Type-I error at level  $\alpha$ . (We refer to this in the benchmarks as the "uniform" test.)

## 2.4 Power against the alternative

While Lemma 1 ensures exact marginal validity of conformal p-values for any deterministic score function  $s$ , the power of the test under the alternative  $H_1 : p \neq q$  crucially depends on how well  $s$  separates samples from  $p$  and  $q$ . A natural and theoretically grounded choice is the *oracle density ratio* between the joint distributions (or equivalently their conditionals for  $\theta$ , since  $p(y) = q(y)$ ). Let  $r(x) = p(x)/q(x)$  denote this true density ratio. If  $\eta(x) := \mathbb{P}(l = 1 \mid x)$  is the output of the Bayes classifier distinguishing between  $x \sim p$  (label  $l = 1$ ) and  $x \sim q$  (label  $l = 0$ ), then the density ratio is related to classifier scores via:

$$r(x) = \frac{\eta(x)}{1 - \eta(x)}. \quad (2)$$

We will soon consider what happens when  $r$  is estimated with error, but for now we suppose it is known. Because the transformation  $t \mapsto t/(1-t)$  is strictly increasing on  $(0, 1)$ , the rankings induced by  $r(x)$  and the probabilities  $\eta(x)$  are identical.

These rankings are of central importance to the conformal method, which depends only on the orderings of scores, not their magnitudes. A natural way to quantify the quality of such a ranking is the area under the ROC curve (AUC) [15], which measures how well a scoring function separates the two distributions. Specifically, the AUC for  $r(x)$  is given by:

$$\text{AUC}(r) = \mathbb{P}_{X \sim p, \tilde{X} \sim q} \left[ r(X) > r(\tilde{X}) \right] + \frac{1}{2} \mathbb{P} \left[ r(X) = r(\tilde{X}) \right],$$

which reflects the probability that a randomly chosen  $p$ -sample is ranked above a  $q$ -sample by the scoring function  $r(x)$ . The next lemma formalizes that  $r(x)$  (or any monotonic transformation of it) maximizes this quantity.

**Lemma 2.** *For any measurable scoring function  $s : \mathcal{X} \rightarrow \mathbb{R}$ ,  $\text{AUC}(s) \leq \text{AUC}(r)$ , with equality if and only if there exists a strictly increasing function  $h$  such that  $s(x) = h(r(x))$  for  $q$ -almost every  $x$ .*

This result justifies the use of the density ratio  $r(x)$  as an optimal scoring function for discriminating between  $p$  and  $q$ ; see Appendix A.1 for the full statement and proof.

Moreover, AUC serves as a useful proxy for the power of the conformal uniformity test, because it quantifies how well the scoring function ranks samples from  $p$  above those from  $q$ . Specifically, as

the number of calibration samples  $m \rightarrow \infty$ , the conformal p-value for a test point  $\tilde{X} \sim q$  converges almost surely to its population-level limit:

$$U \xrightarrow[m \rightarrow \infty]{\text{a.s.}} \mathbb{P}_{X \sim p} [r(X) < r(\tilde{X})] + \xi \mathbb{P}_{X \sim p} [r(X) = r(\tilde{X})], \quad \text{where } \xi \sim \text{Unif}(0, 1).$$

When  $r(x)$  has good separation between the distributions, these p-values tend to concentrate below 0.5, making them detectably non-uniform.

As the number of test points  $n_q \rightarrow \infty$ , the empirical CDF  $\hat{G}(u) = \frac{1}{n_q} \sum_{j=1}^{n_q} \mathbb{I}\{U_j \leq u\}$  converges to the population CDF  $G(u) = \mathbb{P}(U \leq u)$ , and the Kolmogorov–Smirnov test statistic converges to  $\sup_{u \in [0,1]} |G(u) - u|$ , which captures the deviation from uniformity. When AUC exceeds 0.5, i.e.,  $r(x)$  tends to rank  $p$  samples above  $q$ , conformal p-values become stochastically smaller than uniform. This deviation drives up the KS statistic and hence the test power. Moreover, the expected conformal p-value under the alternative is directly related to AUC, as the following lemma establishes.

**Lemma 3.** *Under the alternative  $H_1 : p \neq q$ , we have*

$$\mathbb{E}[U] = 1 - \text{AUC}(r) \leq \frac{1}{2} - \frac{TV(p, q)}{2} < \frac{1}{2}$$

*in the asymptotic limit of  $m \rightarrow \infty$ .*

This result shows that, under the alternative, conformal p-values skew toward zero, with the extent of skewness proportional to the total variation distance between the two distributions. [1] also motivate the density ratio  $r(x) = p(x)/q(x)$  from an information-theoretic perspective, showing that its variability under  $q$  controls the deviation from uniformity; see Lemma 4 in the Appendix.

**Under degraded classifier scores.** Our above analysis involves the oracle density ratio  $r(x)$ . But in practice, the density ratio is often approximated using a classifier trained to distinguish between the true and approximate joint distributions. Accordingly, our analysis explicitly incorporates an error-prone plug-in estimate  $\hat{r}$ , derived from a potentially weak classifier  $\hat{\eta}$  in (2).

Our main theoretical result shows that, under mild regularity conditions on the true and estimated density ratios, the uniform conformal test retains high power, even when the scoring function is imperfect. Our result specifically relates the error of the estimated density ratio to the performance of the conformal C2ST.

**Assumption 1** (Bounded density near zero). *The random variable  $Z := r(\tilde{X}) - r(\tilde{X}')$ , where  $\tilde{X}, \tilde{X}' \stackrel{\text{i.i.d.}}{\sim} q$ , has a density that is bounded in a neighborhood around zero.*

**Assumption 2** ( $L^2$  estimation error). *The estimated density ratio  $\hat{r} : \mathcal{X} \rightarrow (0, \infty)$  satisfies*

$$\mathbb{E}_{\tilde{X} \sim q} [(\hat{r}(\tilde{X}) - r(\tilde{X}))^2] \leq \varepsilon^2,$$

*for some  $\varepsilon > 0$ , where  $r(x) = p(x)/q(x)$  denotes the true density ratio.*

**Theorem 1** (Robustness to estimation error). *Under Assumptions 1 and 2, let  $\hat{U}$  denote the conformal p-value computed using the approximate score function  $\hat{r}$ . Then under the alternative  $H_1 : p \neq q$ , there exists  $M > 0$ , depending on  $\varepsilon$ ,  $p$ , and  $q$ , such that*

$$\mathbb{E}[\hat{U}] - \mathbb{E}[U] \leq \mathcal{O}(\varepsilon^{2/3}) \quad \text{for all } m > M.$$

This theorem shows that the uniform test enjoys a remarkable degree of robustness: even when the classifier is weak or undertrained, the resulting p-values still exhibit systematic deviation from uniformity under the alternative. In particular, the expected p-value computed using an approximate score  $\hat{r}$  remains close to the ideal value obtained from the oracle score  $r$ , with the error controlled by the quality of the approximation. As long as the estimated score preserves a reasonable approximation to the true ranking, the test maintains power. This highlights a key advantage of the conformal approach: it leverages relative score orderings rather than relying on absolute classifier accuracy; We defer the proof to Appendix A.2.

We also emphasize that Assumption 1 is mild and typically satisfied in practice. When  $p$  and  $q$  have overlapping support and the true density ratio  $r(x)$  is smooth, the difference  $Z = r(\tilde{X}) - r(\tilde{X}')$  is a continuous random variable with a density that is finite around zero. This assumption rules out degenerate cases where  $r(x)$  is constant or highly discontinuous, but permits a wide range of practical scenarios in which  $r(x)$  is estimated via smooth classifier outputs. The condition is notably weaker than assuming global Lipschitz continuity of  $r$ .

## 2.5 The multiple test

A potential limitation of the conformal test described above is the need to generate a fresh calibration set for each test point. In many settings, this is not a big issue; drawing from the true joint distribution  $p(\theta, y)$  will often be cheap, as it does not require forward simulation through the generative model. Although repeated calibration does incur multiple passes through the classifier, we find that even a small, low-capacity classifier, so long as it preserves good ranking behavior, can yield competitive results. As a result, the overall computational burden often remains modest.

Nonetheless, we include in our benchmark set an alternative method proposed by [1], which avoids repeated calibration by using a single shared calibration set. This approach is particularly appealing in applications where sampling from  $p$  is expensive, such as when  $p(y | \theta)$  involves a costly forward simulation, since it requires only a single calibration set and avoids repeated draws from the true joint distribution. However, as our experiments show, this convenience comes at the cost of reduced statistical power in some settings.

To correct for the dependence introduced by using a shared calibration set, [1] analyze the average of the conformal p-values computed using a single calibration set as a two-sample U-statistic. They derive an asymptotically valid test statistic by normalizing the deviation of the average p-value from  $1/2$ , which is the expected value under the null. But since we assume the same marginal distribution of  $y$  for both joint distributions, we can simplify their test statistic to obtain:

$$\hat{T} = \frac{\frac{1}{2} - \frac{1}{n_q} \sum_{j=1}^{n_q} \hat{U}_j}{\hat{\sigma} / \sqrt{n_p}} \quad (3)$$

where  $\hat{U}_j := \frac{1}{n_p} \left( \sum_{i=1}^{n_p} \mathbb{I} \left\{ \hat{r}(X_i) < \hat{r}(\tilde{X}_j) \right\} + \xi_j \cdot \sum_{i=1}^{n_p} \mathbb{I} \left\{ \hat{r}(X_i) = \hat{r}(\tilde{X}_j) \right\} \right)$  is obtained from the entire calibration set (common to all test points) with  $\hat{r}(\cdot)$  as the scoring function, and  $\hat{\sigma}$  is the asymptotic estimated standard deviation of  $\frac{\sqrt{n_p}}{n_q} \sum_{j=1}^{n_q} \hat{U}_j$ ; see Appendix A.3 for details. Under the null,  $\hat{T} \sim \mathcal{N}(0, 1)$ , whereas under the alternative,  $\hat{T} \rightarrow \infty$  under the assumptions mentioned in [1, Theorem 2]. Although the original goal of this test was to enhance power under distribution shift, we find that in the NPE setting—where the marginals are matched and classifiers may be weak—the simpler uniform test often yields higher power in practice.

## 3 Experiments

We now empirically evaluate the performance of the conformal C2ST against baseline methods in a scenario with controlled perturbations of a known reference distribution. The experiments are designed to address two key questions. The first concerns *power under proper training*: when the classifier is well trained, how does the conformal C2ST compare to competing methods? The second concerns *robustness to classifier degradation*: as we progressively degrade the quality of the classifier, does the conformal C2ST retain power better than the the ordinary C2ST?

**Controlled posterior perturbations.** To construct a "ground truth" posterior  $p(\theta | y)$ , we proceed following [16]. Let  $y \in \mathbb{R}^k$  and  $\theta \in \mathbb{R}^s$ . We begin by sampling  $y \sim \mathcal{N}(\mathbf{1}_k, I_k)$ , where  $\mathbf{1}_k$  is a vector of ones, and  $I_k$  is the  $k$ -dimensional identity matrix. The conditional distribution  $p(\theta | y)$  is then defined as a multivariate Gaussian,  $p(\theta | y) = \mathcal{N}(\mu_y, \Sigma)$ , where  $\Sigma \in \mathbb{R}^{s \times s}$  is a fixed correlation matrix with entries  $\Sigma_{ij} = 0.9^{|i-j|}$ , introducing structured correlations among the components of  $\theta$ .

Following [16], we introduce controlled perturbations to the reference posterior to construct a notionally "approximate" posterior  $q(\theta | y)$ , with the quality of approximation governed by a scalar parameter  $\gamma \geq 0$ . This framework is well-suited to the neural posterior estimation (NPE) setting, where approximations are learned from simulation and common failure modes—such as biased means, miscalibrated variances, or structural misspecifications—can arise due to limited model capacity or suboptimal training. By explicitly designing perturbations that reflect these modes of failure, we can assess whether a testing method reliably detects meaningful discrepancies between the true posterior  $p(\theta | y)$  and its perturbed counterpart. When  $\gamma = 0$ , we recover the true posterior; increasing  $\gamma$  yields progressively less faithful approximations.

Below, we include the following four perturbations from [16] here and defer the rest to Appendix B.

- **Covariance Scaling.** To model over- or under-confidence in uncertainty quantification, we uniformly inflate (or deflate) the covariance matrix:  $q(\theta | y) = \mathcal{N}(\mu_y, (1 + \gamma)\Sigma_y)$ . This captures calibration failures where the posterior has the correct shape and center but misrepresents its overall spread.
- **Anisotropic Covariance Perturbation.** We introduce structured distortion in the posterior shape by injecting uncertainty along the direction of least variance:  $q(\theta | y) = \mathcal{N}(\mu_y, \Sigma_y + \gamma\Delta)$ , where  $\Delta = \mathbf{v}_{\min}\mathbf{v}_{\min}^\top$  and  $\mathbf{v}_{\min}$  is the eigenvector of  $\Sigma_y$  corresponding to its smallest eigenvalue. This subtly alters the posterior geometry.
- **Heavy-Tailed Perturbation.** To explore deviations in tail behavior, we replace the Gaussian with a multivariate  $t$ -distribution:  $q(\theta | y) = t_\nu(\mu_y, \Sigma_y)$  where  $\nu = 1/(\gamma + \epsilon)$ . As  $\gamma \rightarrow 0$ , the distribution approaches Gaussian; increasing  $\gamma$  yields heavier tails, modeling posterior approximations that spuriously introduce more extreme values.
- **Mode Collapse.** We introduce a symmetric mode in the true posterior with weight  $\gamma$ , so that  $p(\theta | y) = \gamma\mathcal{N}(-\mu_y, \Sigma_y) + (1 - \gamma)\mathcal{N}(\mu_y, \Sigma_y)$  while  $q(\theta | y) = \mathcal{N}(\mu_y, \Sigma_y)$ . As  $\gamma \rightarrow 0$ , the two match, while increasing  $\gamma$  increases the mass of the missed mode.

**Testing classifier degradation.** After training a classifier on a given benchmark problem at a fixed perturbation level  $\gamma$ , we then generate a family of degraded classifiers by linearly interpolating the trained model parameters with those of a randomly initialized model:

$$\psi_\beta := (1 - \beta) \cdot \psi_{\hat{\eta}} + \beta \cdot \psi_{\text{rand}}, \quad \beta \in [0, 1],$$

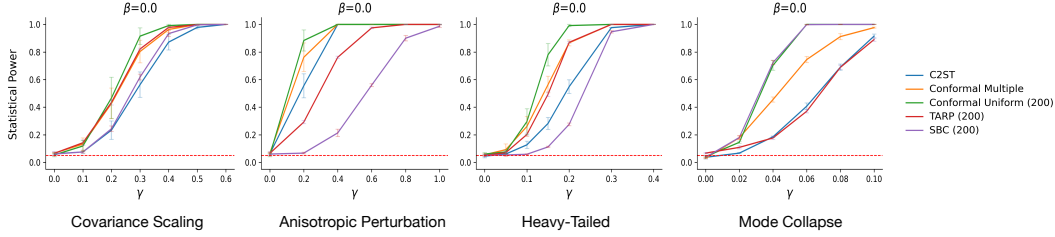
where  $\psi_{\hat{\eta}}$  and  $\psi_{\text{rand}}$  are the parameter vectors of the trained and randomly initialized classifiers, respectively. This setup allows us to systematically degrade the classifier’s quality by varying  $\beta$ , from a fully trained model ( $\beta = 0$ ) to a random, uninformative one ( $\beta = 1$ ). Class probabilities and nonconformity scores are calculated from the degraded classifier. We then evaluate the behavior of both the standard C2ST and the conformal C2ST across this interpolation path. This experiment provides a natural stress test for the conformal framework. If the conformal method maintains detection power even as the classifier degrades, this would offer compelling evidence of its practical robustness. We note that this experiment is specific to classifier-based testing methods; approaches like SBC and TARP, which do not involve classifiers, are not applicable in this setting.

**Experiment settings and baselines.** We benchmark the conformal C2ST against several well-established methods for assessing the quality of a neural posterior estimate. These include the *Classifier Two-Sample Test (C2ST)* [11], described in Section 2.1; *Simulation-Based Calibration (SBC)* [9], which computes rank statistics for each marginal of  $q(\theta | y)$  and checks for uniformity under the true posterior; and *TARP (Tests of Accuracy with Random Points)* [10], which uses randomly sampled reference points and distance-based statistics to construct a test that is both necessary and sufficient for posterior validity.

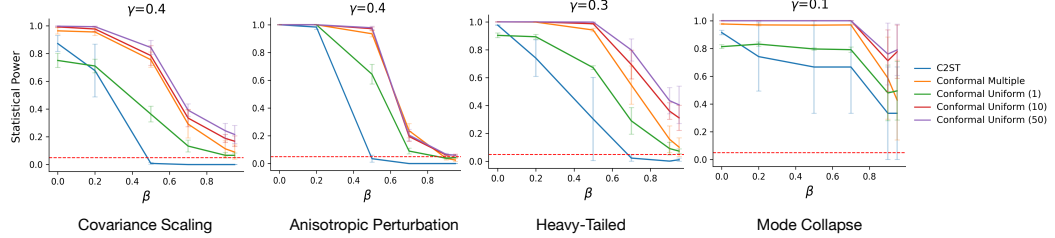
We adapt each baseline method as follows. For C2ST, given each  $y$  sample, we sample once from  $q(\theta | y)$  to create balanced training and test datasets. For SBC, we sample  $m$  posterior samples from the approximate posterior for each  $y$ , then conduct the KS test between the rank statistics and the uniform distribution for each dimension independently, followed by Bonferroni correction to control for multiple testing. For TARP, we select random reference points and use the internal variables of its procedure to perform a KS test against the uniform distribution. Further implementation details and design choices are deferred to Appendix B.2. For the conformal C2ST method, we evaluate both the "uniform test" from Section 2.2, as well the "multiple test" variant described by [1], from Section 2.5.

For all tests, we set the significance threshold at  $\alpha = 0.05$ . For each experiment, we sample 1000 labeled data points  $\{y_i, \theta_i, 1\}$  and  $\{\tilde{y}_i, \tilde{\theta}_i, 0\}$  each from the true ( $p$ ) and approximate ( $q$ ) joint distributions, and we train a neural network classifier to discriminate between them. Then during testing, we evaluate the test power or Type I error by sampling 200 additional batches with the same sampling budget as in training. All experiments are repeated with three random seeds, and we report the average results. Further details regarding training procedures and hyperparameters are provided in Appendix B.1.

In our experiments with the uniformity test, we take advantage of the fact that samples from the true joint distribution  $p(\theta, y)$  are typically cheap to generate in the NPE setting. For each test point drawn from the approximate posterior  $q$ , we sample  $m$  calibration points from  $p$ , resulting in a total of



(a) Power curves as a function of perturbation level  $\gamma$  at fixed classifier quality ( $\beta = 0$ ).



(b) Power curves as a function of classifier degradation level  $\beta$  at fixed perturbation strength  $\gamma$ .

Figure 2: Statistical power of C2ST and conformal variants across benchmark perturbations. Panel (a) evaluates sensitivity to posterior mismatch; panel (b) evaluates robustness to classifier degradation.

$m \cdot 1000$  labeled samples from  $p$  (with label 1), and 1000 labeled samples from  $q$  (with label 0). We refer to this configuration as **Conformal Uniform**( $m$ ), where  $m \in \{1, 2, 5, 10, 20, 50, 200\}$  controls the number of calibration points per test point used to calculate conformal p-values. Increasing  $m$  generally improves the power of the test, since more calibration samples yield more accurate p-values and finer resolution for detecting deviations from uniformity. For an empirical study of how test performance varies with  $m$ , see the ablation experiments in Appendix B.3.

**Results.** We summarize the performance of the testing methods across two complementary experiments, with more dimensionality settings considered in the Appendix. In the first experiment (Figure 2a), we vary the perturbation strength  $\gamma$  while keeping the classifier fully trained ( $\beta = 0$ ), to assess how sensitive each method is to deviations from the true posterior. Across all perturbation types, we find that conformal methods match or exceed the performance of SBC and TARP, while consistently achieving higher power than the standard C2ST baseline. In particular, Conformal Uniform(200) and Conformal Multiple detect even subtle deviations at low values of  $\gamma$ . While all methods eventually reach near-perfect power as the perturbation strength increases, conformal methods offer earlier detection thresholds, especially in the covariance scaling and anisotropic perturbation cases.

In the second experiment (Figure 2b), we fix  $\gamma$  and degrade the classifier by interpolating its parameters with those of a randomly initialized model, increasing  $\beta$  from 0 to 1. The power of the C2ST drops off sharply with increasing  $\beta$ , falling to near-random levels even at moderate degradation. In contrast, the conformal variants degrade much more slowly. Conformal Uniform(10, 50) and Conformal Multiple maintain high power throughout most of the degradation path, while Conformal Uniform(1) also outperforms C2ST, though with somewhat reduced robustness. These results demonstrate that conformal methods are significantly less sensitive to classifier quality, due to their reliance on score rankings rather than absolute accuracy. The code is available at [https://github.com/TianyuCodings/conformal\\_c2st](https://github.com/TianyuCodings/conformal_c2st).

**Limitations.** Our benchmarking framework benefits from cheap access to  $p(y | \theta)$ , which may not be available in many NPE settings where the data arises from a black-box simulation model. While this enables rigorous evaluation in controlled experiments, it limits applicability to certain types of NPE scenarios. In our theoretical analysis, we rely on bounding arguments that may be conservative; tighter analytical techniques could potentially yield sharper error bounds and offer a more precise characterization of test behavior.

## References

- [1] Xiaoyu Hu and Jing Lei. A two-sample conditional distribution test using conformal prediction and weighted rank sum. *Journal of the American Statistical Association*, 119(546):1136–1154, 2024. doi: 10.1080/01621459.2023.2177165. URL <https://doi.org/10.1080/01621459.2023.2177165>.
- [2] Jonathan Ho, Ajay Jain, and Pieter Abbeel. Denoising diffusion probabilistic models. *Advances in neural information processing systems*, 33:6840–6851, 2020.
- [3] Tomas Geffner, George Papamakarios, and Andriy Mnih. Compositional score modeling for simulation-based inference. In *International Conference on Machine Learning*, pages 11098–11116. PMLR, 2023.
- [4] Tianyu Chen, Vansh Bansal, and James G Scott. Conditional diffusions for amortized neural posterior estimation. In *International Conference on Artificial Intelligence and Statistics*, pages 2377–2385. PMLR, 2025.
- [5] Manuel Gloeckler, Michael Deistler, Christian Weilbach, Frank Wood, and Jakob H Macke. All-in-one simulation-based inference. *arXiv preprint arXiv:2404.09636*, 2024.
- [6] George Papamakarios, Eric Nalisnick, Danilo Jimenez Rezende, Shakir Mohamed, and Balaji Lakshminarayanan. Normalizing flows for probabilistic modeling and inference. *Journal of Machine Learning Research*, 22(57):1–64, 2021.
- [7] Jonas Wildberger, Maximilian Dax, Simon Buchholz, Stephen Green, Jakob H Macke, and Bernhard Schölkopf. Flow matching for scalable simulation-based inference. *Advances in Neural Information Processing Systems*, 36:16837–16864, 2023.
- [8] Diederik P Kingma, Max Welling, et al. Auto-encoding variational bayes, 2013.
- [9] Sean Talts, Michael Betancourt, Daniel Simpson, Aki Vehtari, and Andrew Gelman. Validating bayesian inference algorithms with simulation-based calibration. *arXiv preprint arXiv:1804.06788*, 2018.
- [10] Pablo Lemos, Adam Coogan, Yashar Hezaveh, and Laurence Perreault-Levasseur. Sampling-based accuracy testing of posterior estimators for general inference. In *International Conference on Machine Learning*, pages 19256–19273. PMLR, 2023.
- [11] David Lopez-Paz and Maxime Oquab. Revisiting classifier two-sample tests. *arXiv preprint arXiv:1610.06545*, 2016.
- [12] Vladimir Vovk, Alex Gamerman, and Glenn Shafer. *Algorithmic Learning in a Random World*. Springer, 2005.
- [13] Jing Lei and Max G’Sell. Distribution-free predictive inference for regression. *Journal of the American Statistical Association*, 113(523):1094–1111, 2018.
- [14] E. L. Lehmann and Joseph P. Romano. *Testing Statistical Hypotheses*. Springer Texts in Statistics. Springer, New York, 3rd edition, 2005. ISBN 0-387-98864-5.
- [15] Tom Fawcett. An introduction to roc analysis. *Pattern Recognition Letters*, 27(8):861–874, 2006.
- [16] Tianyu Chen, Vansh Bansal, and James Scott. NPTBench: A benchmark suite for neural posterior testing. Technical report, 2024. URL <https://github.com/TianyuCodings/NPTBench>.
- [17] Laurent Dinh, Jascha Sohl-Dickstein, and Samy Bengio. Density estimation using real nvp. *arXiv preprint arXiv:1605.08803*, 2016.

## A Theoretical Results

In this section, we restate our key lemmas in full and provide rigorous proofs to support our theoretical claims.

### A.1 Proofs of Lemma 2 and 3

**Lemma 2** (Full statement). *Let  $p$  and  $q$  be two probability densities on a measurable space  $\mathcal{X}$ , such that  $p(x) > 0$  and  $q(x) > 0$  for all  $x \in \mathcal{X}$ . Let  $r(x) := \frac{p(x)}{q(x)}$  denote the oracle density ratio. For any measurable scoring function  $s : \mathcal{X} \rightarrow \mathbb{R}$ , define the area under the ROC curve (AUC) as*

$$\text{AUC}(s) := \mathbb{P}[s(X) > s(\tilde{X})] + \frac{1}{2}\mathbb{P}[s(X) = s(\tilde{X})],$$

where  $X \sim p$  and  $\tilde{X} \sim q$  are independent.

Then  $\text{AUC}(s) \leq \text{AUC}(r)$ , with equality if and only if there exists a strictly increasing function  $h$  such that  $s(x) = h(r(x))$  for  $p \times q$ -almost every  $x$ .

*Proof.* Define

$$\phi_s(x, \tilde{x}) := \mathbb{I}[s(x) > s(\tilde{x})] + \frac{1}{2}\mathbb{I}[s(x) = s(\tilde{x})],$$

so that

$$\text{AUC}(s) = \iint \phi_s(x, \tilde{x}) p(x)q(\tilde{x}) dx d\tilde{x}.$$

Define the antisymmetric part

$$a_s(x, \tilde{x}) := \phi_s(x, \tilde{x}) - \phi_s(\tilde{x}, x) \in \{-1, 0, 1\}.$$

Note that  $\phi_s(x, \tilde{x}) + \phi_s(\tilde{x}, x) = 1$ , hence

$$\phi_s(x, \tilde{x}) = \frac{1}{2} + \frac{1}{2}a_s(x, \tilde{x}),$$

and therefore

$$\text{AUC}(s) = \frac{1}{2} + \frac{1}{2} \iint a_s(x, \tilde{x}) p(x)q(\tilde{x}) dx d\tilde{x}.$$

Define the antisymmetric function

$$W(x, \tilde{x}) := p(x)q(\tilde{x}) - p(\tilde{x})q(x),$$

so that

$$\iint a_s(x, \tilde{x}) p(x)q(\tilde{x}) dx d\tilde{x} = \frac{1}{2} \iint a_s(x, \tilde{x}) W(x, \tilde{x}) dx d\tilde{x},$$

and thus

$$\text{AUC}(s) = \frac{1}{2} + \frac{1}{4} \iint a_s(x, \tilde{x}) W(x, \tilde{x}) dx d\tilde{x}.$$

Now for each  $(x, \tilde{x})$ , the value  $a_s(x, \tilde{x}) \in \{-1, 0, 1\}$  that maximizes the product  $a_s(x, \tilde{x})W(x, \tilde{x})$  is  $\text{sign}(W(x, \tilde{x}))$ . Therefore, the function

$$a^*(x, \tilde{x}) := \text{sign}(W(x, \tilde{x}))$$

maximizes the integral.

Next, define the likelihood ratio  $r(x) := \frac{p(x)}{q(x)}$ . Then

$$r(x) > r(\tilde{x}) \iff \frac{p(x)}{q(x)} > \frac{p(\tilde{x})}{q(\tilde{x})} \iff p(x)q(\tilde{x}) > p(\tilde{x})q(x) \iff W(x, \tilde{x}) > 0,$$

so

$$a_r(x, \tilde{x}) := \text{sign}(r(x) - r(\tilde{x})) = \text{sign}(W(x, \tilde{x})) = a^*(x, \tilde{x}).$$

Thus,  $a_r$  maximizes the integral, and

$$\text{AUC}(s) \leq \frac{1}{2} + \frac{1}{4} \iint |W(x, \tilde{x})| dx d\tilde{x} = \text{AUC}(r).$$

Finally, equality occurs if and only if  $a_s(x, \tilde{x}) = a_r(x, \tilde{x})$  for almost all  $(x, \tilde{x})$ , which implies that  $s(x) > s(\tilde{x}) \iff r(x) > r(\tilde{x})$ , i.e.,  $s = h(r)$  for some strictly increasing function  $h$  almost everywhere.  $\square$

**Corollary 1** (Lower Bound on AUC via Total Variation). *Under the setup of the previous lemma, let  $\text{TV}(p, q) := \frac{1}{2} \int |p(x) - q(x)| dx$  denote the total variation distance between  $p$  and  $q$ . Then*

$$\text{AUC}(r) \geq \frac{1 + \text{TV}(p, q)}{2}.$$

*Proof.* Consider the binary Bayes classifier

$$\phi^*(x) := \mathbb{I}[r(x) > 1] = \mathbb{I}\left[\frac{p(x)}{q(x)} > 1\right],$$

which is known to be the most powerful test at level  $\alpha = \frac{1}{2}$ . Its classification accuracy is:

$$\mathbb{P}[\phi^*(X) = 1] \cdot \frac{1}{2} + \mathbb{P}[\phi^*(\tilde{X}) = 0] \cdot \frac{1}{2} = \frac{1}{2} + \frac{1}{2} \text{TV}(p, q).$$

Now note that if we treat  $\phi^* \in \{0, 1\}$  as a scoring function, the AUC of this classifier is:

$$\text{AUC}(\phi^*) = \mathbb{P}[\phi^*(X) > \phi^*(\tilde{X})] + \frac{1}{2} \mathbb{P}[\phi^*(X) = \phi^*(\tilde{X})] \leq \text{AUC}(r),$$

since  $\phi^*$  is a thresholding of  $r$ , and AUC is maximized by ranking with  $r$ .

But:

$$\text{AUC}(\phi^*) = \frac{1}{2} + \frac{1}{2} \text{TV}(p, q),$$

so we conclude:

$$\text{AUC}(r) \geq \frac{1}{2} + \frac{1}{2} \text{TV}(p, q) = \frac{1 + \text{TV}(p, q)}{2}.$$

$\square$

**Lemma 3** (Expected conformal p-value under the alternative). *Let  $p$  and  $q$  be as defined above, and let  $U$  denote the conformal p-value computed using the oracle density ratio  $r(x) = p(x)/q(x)$  as the score function, as defined in (1), with  $m$  calibration samples drawn from  $p$  for each test point drawn from  $q$ . Then, under the alternative hypothesis  $H_1 : p \neq q$ , we have*

$$\mathbb{E}[U] = 1 - \text{AUC}(r) \leq \frac{1}{2} - \frac{1}{2} \text{TV}(p, q) < \frac{1}{2},$$

in the limit as  $m \rightarrow \infty$ .

*Proof.* We formalize our discussion in Section 2.4. First, by the strong law of large numbers, we have

$$U \xrightarrow[m \rightarrow \infty]{\text{a.s.}} \mathbb{P}_{X \sim p} [r(X) < r(\tilde{X})] + \xi \mathbb{P}_{X \sim p} [r(X) = r(\tilde{X})], \quad \text{where } \xi \sim \text{Unif}(0, 1).$$

Next, we take expectation with respect to  $\tilde{X} \sim q$  and  $\xi \sim \text{Unif}(0, 1)$ . However, since  $U \leq 1$ , Dominated Convergence Theorem gives that

$$\begin{aligned} \mathbb{E}[U] &\xrightarrow[m \rightarrow \infty]{\text{a.s.}} \mathbb{P} [r(X) < r(\tilde{X})] + \frac{1}{2} \mathbb{P} [r(X) = r(\tilde{X})] \\ &= 1 - \text{AUC}(r) \end{aligned}$$

The result follows immediately from Corollary 1, since  $0 < \text{TV}(p, q) \leq 1$  under  $H_1 : p \neq q$ .  $\square$

We note that [1] present a related result from an information-theoretic perspective, showing that the variability of the density ratio  $r(x)$  under  $q$  controls the deviation of conformal p-values from uniformity. In contrast, our focus is on quantifying the relationship between a classifier's discriminative ability and the statistical power of the resulting two-sample test. While the underlying intuition is similar, our formulation offers a more direct and operational perspective, grounded in the ranking statistic captured by the AUC score. For completeness, we restate their relevant lemma below.

**Lemma 4** (Restated from [1]). *Under the alternative  $H_1 : p \neq q$ , we have*

$$\mathbb{E}[U] = \frac{1}{2} - \frac{1}{4} \mathbb{E}_{X, X' \sim q} [|r(X) - r(X')|] < \frac{1}{2} \quad \text{as } m \rightarrow \infty,$$

where  $X, X'$  are i.i.d. draws from  $q$ .

## A.2 Proof of Theorem 1

*Proof.* We start by taking the expectation of our conformal p-value wrt the tie breaking uniform variable  $\xi$ :

$$2 \mathbb{E}_\xi[\hat{U}] = \frac{1}{m+1} \left( \sum_{i=1}^m \mathbb{I}(\hat{r}(X_i) < \hat{r}(\tilde{X})) + \sum_{i=1}^m \mathbb{I}(\hat{r}(X_i) \leq \hat{r}(\tilde{X})) + 1 \right).$$

By the Strong Law of Large Numbers (SLLN), as  $m \rightarrow \infty$ , we have:

$$2 \mathbb{E}_\xi[\hat{U}] \rightarrow \mathbb{E}[\mathbb{I}(\hat{r}(X) < \hat{r}(\tilde{X})) \mid \tilde{X}] + \mathbb{E}[\mathbb{I}(\hat{r}(X) \leq \hat{r}(\tilde{X})) \mid \tilde{X}].$$

Taking expectation over  $\tilde{X}$  and applying the Dominated Convergence Theorem (since  $\hat{U} \leq 1$ ):

$$2 \mathbb{E}[\hat{U}] \rightarrow \mathbb{E}[\mathbb{I}(\hat{r}(X) < \hat{r}(\tilde{X}))] + \mathbb{E}[\mathbb{I}(\hat{r}(X) \leq \hat{r}(\tilde{X}))].$$

Now define  $\tilde{X}, \tilde{X}' \stackrel{\text{iid}}{\sim} q$ . Using importance reweighting, we write:

$$2 \mathbb{E}[\hat{U}] = \mathbb{E} \left[ r(\tilde{X}') \cdot \mathbb{I}(\hat{r}(\tilde{X}') < \hat{r}(\tilde{X})) \right] + \mathbb{E} \left[ r(\tilde{X}') \cdot \mathbb{I}(\hat{r}(\tilde{X}') \leq \hat{r}(\tilde{X})) \right].$$

Since  $\mathbb{E}[r(\tilde{X}')] = 1$ , this becomes:

$$2 \mathbb{E}[\hat{U}] = 1 - \mathbb{E}[(r(\tilde{X}') - r(\tilde{X})) \cdot \mathbb{I}(\hat{r}(\tilde{X}') > \hat{r}(\tilde{X}))].$$

Define:

$$Z := r(\tilde{X}') - r(\tilde{X}), \quad \hat{Z} := \hat{r}(\tilde{X}') - \hat{r}(\tilde{X}), \quad \Delta := \hat{Z} - Z.$$

Then:

$$\mathbb{E}[\hat{U}] = \mathbb{E}[U] + \frac{1}{2} \delta, \quad \text{where } \delta := \frac{1}{2} \mathbb{E}[|Z|] - \mathbb{E}[Z \cdot \mathbb{I}(\hat{Z} > 0)].$$

By symmetry of  $Z$ ,

$$\delta = \frac{1}{2} \mathbb{E}[|Z|] - \mathbb{E}[Z \cdot \mathbb{I}(\hat{Z} > 0)] = \mathbb{E}[Z(\mathbb{I}(Z > 0) - \mathbb{I}(\hat{Z} > 0))].$$

Define events:

$$A := \{Z > 0, \hat{Z} \leq 0\}, \quad B := \{Z \leq 0, \hat{Z} > 0\}.$$

Then:

$$\delta = \mathbb{E}[Z \cdot \mathbb{I}_A] - \mathbb{E}[Z \cdot \mathbb{I}_B] \leq \mathbb{E}[|Z| \cdot \mathbb{I}_{|\Delta| \geq |Z|}].$$

For any threshold  $t > 0$ , we decompose:

$$\delta \leq \mathbb{E}[|Z| \cdot \mathbb{I}(|Z| \leq t)] + \mathbb{E}[|Z| \cdot \mathbb{I}(|\Delta| > t)].$$

The second term is bounded by Cauchy–Schwarz and Markov:

$$\mathbb{E}[|Z| \cdot \mathbb{I}(|\Delta| > t)] \leq \sqrt{\mathbb{E}[Z^2]} \cdot \sqrt{\mathbb{P}(|\Delta| > t)} \leq \sqrt{\mathbb{E}[Z^2]} \cdot \frac{2\varepsilon}{t}.$$

Assuming the density  $f_Z$  of  $Z$  is bounded near zero by  $C$ , we have:

$$\mathbb{E}[|Z| \cdot \mathbb{I}(|Z| \leq t)] \leq 2C \int_0^t z dz = Ct^2.$$

Combining,

$$\delta \leq Ct^2 + \frac{2\sqrt{\mathbb{E}[Z^2]}\varepsilon}{t}.$$

Minimizing the RHS by choosing  $t = \left(\frac{2\sqrt{\mathbb{E}[Z^2]}\varepsilon}{C}\right)^{1/3}$ , we obtain:

$$\delta = O(\varepsilon^{2/3}).$$

□

### A.3 Multiple test details

In this section, we summarize the multiple conformal testing procedure proposed by [1], which accounts for the dependence among p-values arising from the use of a shared calibration set. Under the NPE setting, where the marginal distribution of  $y$  is assumed to be the same under both the true and approximate joint distributions, we derive a simplified form of their test statistic:

$$\hat{T} = \frac{\frac{1}{2} - \frac{1}{n_q} \sum_{j=1}^{n_q} \hat{U}_j}{\hat{\sigma} / \sqrt{n_p}}$$

where  $\hat{U}_j := \frac{1}{n_p} \left( \sum_{i=1}^{n_p} \mathbb{I} \left\{ \hat{r}(X_i) < \hat{r}(\tilde{X}_j) \right\} + \xi_j \cdot \sum_{i=1}^{n_p} \mathbb{I} \left\{ \hat{r}(X_i) = \hat{r}(\tilde{X}_j) \right\} \right)$  is obtained from the entire calibration set (common to all test points) with  $\hat{r}(\cdot)$  as the scoring function, and  $\hat{\sigma}$  is the asymptotic estimated standard deviation of  $\frac{\sqrt{n_p}}{n_q} \sum_{j=1}^{n_q} \hat{U}_j$ . We also adapt their expression for the variance estimate to the same-marginal setting. Let  $\hat{F}$  be the empirical CDF of  $\left\{ \hat{r}(\tilde{X}_j) : j \in [n_q] \right\}$  and  $\hat{F}_-$  be its left limit. Then the variance estimate is given by:

$$\hat{\sigma}^2 = \hat{\sigma}_1^2 + \frac{n_p}{12 \cdot n_q}$$

where  $\hat{\sigma}_1^2$  is the empirical variance of  $\left\{ \hat{F}_{1/2}(\hat{r}(X_i)) : i \in [n_p] \right\}$  and  $\hat{F}_{1/2}(t) = \left( \hat{F}(t) + \hat{F}_-(t) \right) / 2$ .

## B Experiment Details

### B.1 Training Details

We use a three-layer neural network classifier with skip connections and a hidden dimension of 256. The network is initialized using PyTorch’s default parameter initialization. Optimization is performed using the Adam optimizer with a cosine annealing learning rate schedule.

The training set consists of 2,000 samples: 1,000 labeled examples of the form  $\{y_i, \theta_i, 1\}$ , drawn from the joint distribution  $p(\theta | y)p(y)$ , and 1,000 negative examples from  $q(\theta | y)p(y)$ . Each pair  $(\theta, y)$  lies in  $\mathbb{R}^{3 \times 3}$ . We train the model for 2,000 epochs using a fixed learning rate of  $1 \times 10^{-5}$ , which is sufficient to ensure convergence in our experiments.

### B.2 Evaluation Details

For evaluation, using the trained classifier, we sample  $1000 \cdot m$  data points  $\{y_i, \theta_i\}$  from  $p(\theta | y)p(y)$ , and another 1,000 samples from  $q(\theta | y)p(y)$  to compute the rejection rate for C2ST and its conformal variants.

For classical C2ST and the Conformal Multiple testing variant, we set  $k = 1$ . For the Conformal Uniform test, we vary  $k \in \{1, 2, 5, 10, 20, 50, 200\}$ . We denote this setting as **Conformal Uniform**( $k$ ), where  $k$  specifies the evaluation sample budget.

For SBC and TARP, which require multiple posterior samples per observation  $y$ , we draw 200 posterior samples  $\theta$  for each  $y$ . The overall evaluation budget remains consistent, using 1,000 pairs  $(y, \theta)$  from  $p(\theta | y)p(y)$ . We denote these methods as **SBC(200)** and **TARP(200)** to indicate the number of posterior samples used.

To ensure a fair comparison, we report results for C2ST, Conformal Multiple testing, Conformal Uniform(200), SBC(200), and TARP(200) when evaluating the statistical power of our method.

### B.3 Additional experiment results with perturbed Gaussians

Below, we include two additional perturbations from [16] other than the ones mentioned in Section 3 of the main text.

- **Mean Shift.** To simulate systematic location bias, we perturb the posterior mean while keeping the covariance fixed:  $q(\theta | y) = \mathcal{N}((1 + \gamma)\mu_y, \Sigma_y)$ . This mimics scenarios where the NPE model consistently misses the location of the true posterior mode.
- **Additional Mode.** We introduce a symmetric mode in the approximate posterior with weight  $\gamma$ , so that  $q(\theta | y) = \gamma \mathcal{N}(-\mu_y, \Sigma_y) + (1 - \gamma) \mathcal{N}(\mu_y, \Sigma_y)$  while  $p(\theta | y) = \mathcal{N}(\mu_y, \Sigma_y)$ . As  $\gamma \rightarrow 0$ , the two match, while increasing  $\gamma$  increases the mass of the spurious mode.

Figures 5 to 10 present our experimental results, comparing our proposed methods against the baselines and including ablations on the number of calibration samples used in the conformal uniform test. Across all perturbation types, we observe consistent improvements over the classical C2ST under classifier degradation, highlighting the robustness of our method.

## C Experiments on high dimensional posteriors with manifold structure

We further evaluate robustness and calibration of the proposed conformal tests in settings where the true posterior lies on a low-dimensional manifold embedded in a high-dimensional space. Specifically, we construct synthetic posteriors using a conditional normalizing flow model trained on data generated from a nonlinear spherical manifold, enabling controlled perturbations and precise comparisons across methods.

**Problem setup.** We first sample  $n$  points uniformly on the surface of the unit sphere in  $\mathbb{R}^3$  using spherical coordinates  $\phi \sim \mathcal{U}[0, \pi]$ ,  $\tau \sim \mathcal{U}[0, 2\pi]$ , and convert them to Cartesian coordinates:

$$a = \sin(\phi) \cos(\tau), \quad b = \sin(\phi) \sin(\tau), \quad c = \cos(\phi).$$

These coordinates are mapped into a higher-dimensional ambient space  $\mathbb{R}^d$  (with  $d = 100$ ) via a random projection matrix  $W \in \mathbb{R}^{3 \times d}$  sampled from a standard Gaussian, yielding

$$\theta = W^\top (a, b, c)^\top + \varepsilon, \quad \varepsilon \sim \mathcal{N}(0, \sigma^2 I),$$

where  $\theta \in \mathbb{R}^d$  and  $\sigma > 0$  controls the noise level. The corresponding conditioning variable is defined as  $y = (\phi/\pi, \tau/2\pi)$ , so that  $y \in [0, 1]^2$ .

**Training details.** We simulate posterior distributions using a conditional normalizing flow (CNF) model based on RealNVP [17]. Our architecture consists of 8 RealNVP layers, each parameterized by a neural network with one hidden layer of width 512. The model is trained for 500 epochs to ensure convergence. The true posterior is obtained by applying the inverse flow to a base sample  $z \sim \mathcal{N}(\gamma, I)$ , where  $\gamma = 0$ .

To simulate an approximate posterior, we perturb the base distribution by introducing a mean shift  $\gamma \in \mathbb{R}^d$ , such that  $z \sim \mathcal{N}(\gamma, I)$  instead of the true  $z \sim \mathcal{N}(0, I)$ . The resulting approximate posterior  $q(\theta | y)$  is thus generated by applying the same flow model to this mis-specified base distribution.

Figure 3 illustrates samples from the true and approximate posteriors for various values of  $\gamma$ , projected onto the first two principal components using Principal Component Analysis (PCA).

To distinguish between the true and approximate posteriors, we compute log density ratios by subtracting the log-probabilities assigned by the two CNF models. To emulate degradation in the classifier’s discriminative ability, we add Gaussian noise  $\delta \sim \mathcal{N}(0, \beta^2)$  to the log-density ratios. When  $\beta = 0$ , the scores are exact; as  $\beta$  increases, the scores become progressively noisier, reflecting reduced discriminative power. Figure 4 shows that conformal variants of C2ST outperform all baselines under increasing posterior perturbation and retain a better test power under classifier degradation.

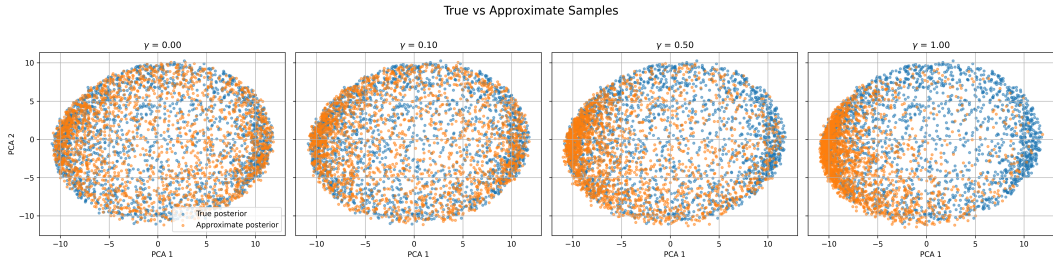
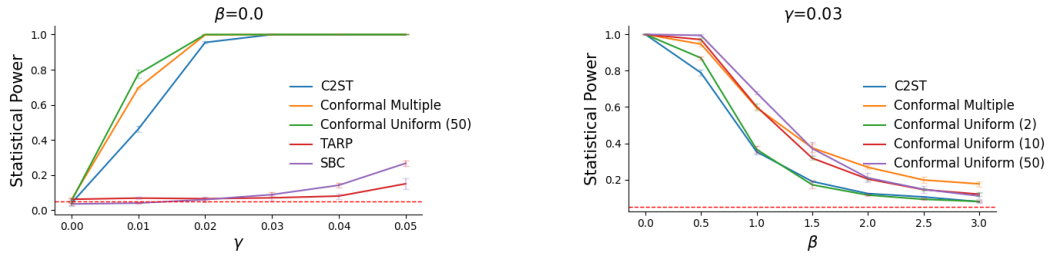


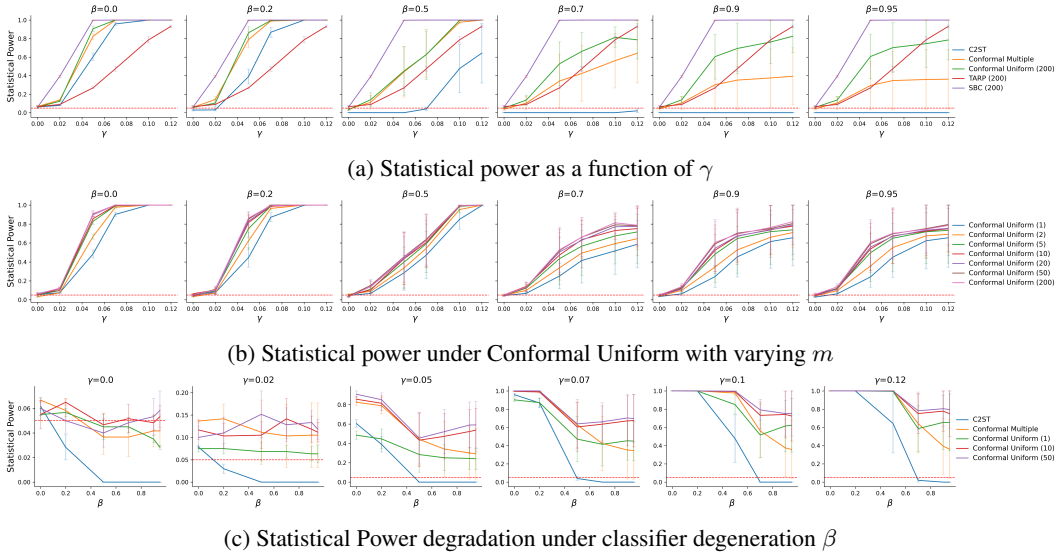
Figure 3: Approximate posterior samples (as a function of the base mean perturbation  $\gamma$ ) projected on the first two principal axes



(a) Statistical power as a function of base mean perturbation  $\gamma$

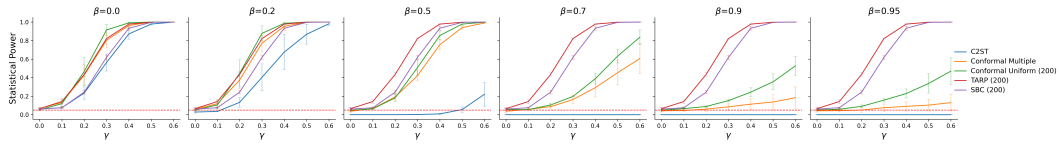
(b) Statistical power as a function of classifier noise  $\beta$

Figure 4: Power analysis under mean perturbation of the base distribution of the normalizing flow model.

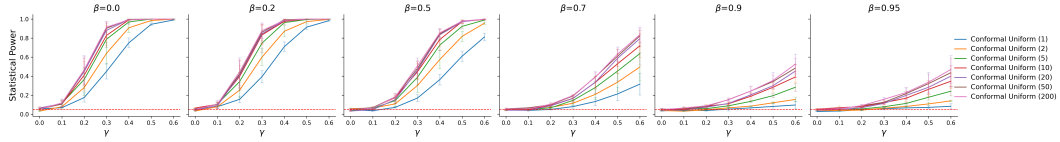


(c) Statistical Power degradation under classifier degeneration  $\beta$

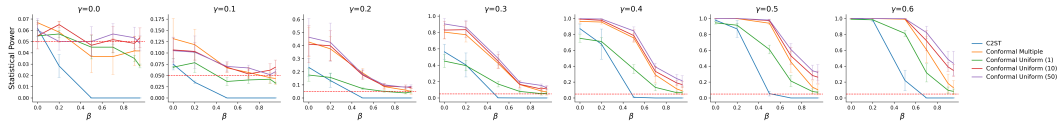
Figure 5: Power analysis under Mean Shift



(a) Statistical power as a function of  $\gamma$

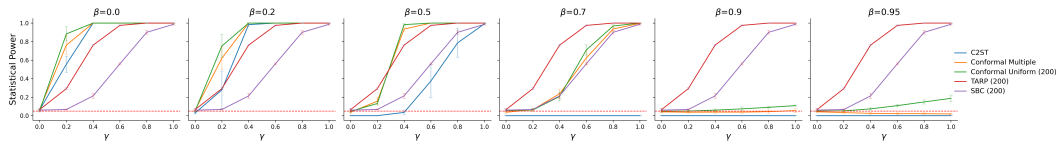


(b) Statistical power under Conformal Uniform with varying  $m$

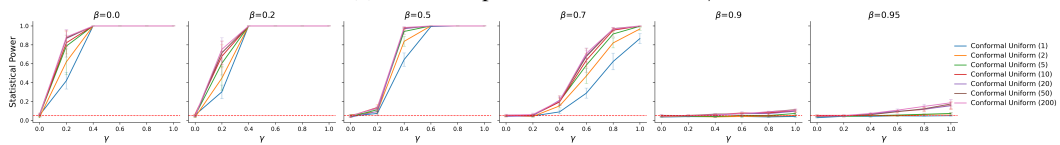


(c) Statistical Power degradation under classifier degeneration

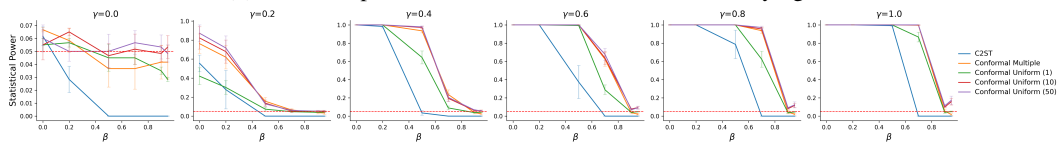
Figure 6: Power analysis under Covariance Scaling.



(a) Statistical power as a function of  $\gamma$

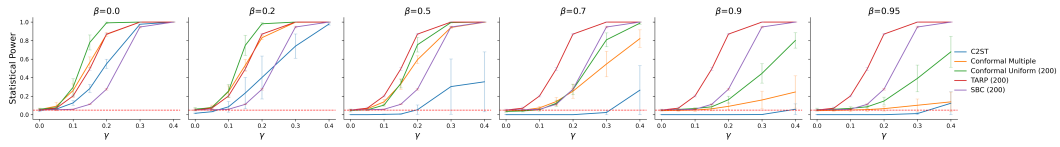


(b) Statistical power under Conformal Uniform with varying  $m$ .

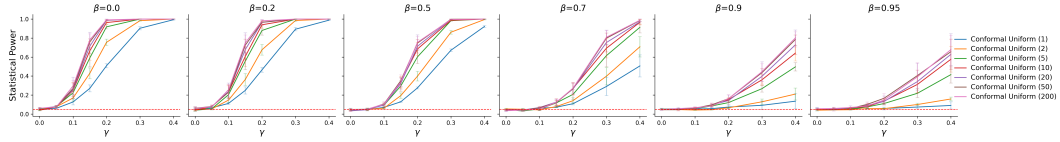


(c) Statistical Power degradation under classifier degeneration

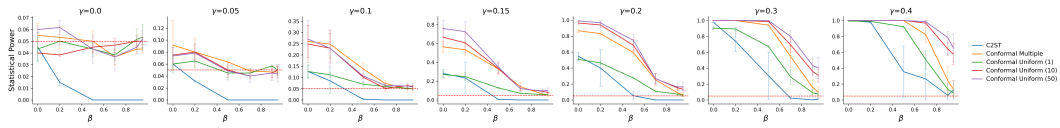
Figure 7: Power analysis under Anisotropic Covariance Perturbation.



(a) Statistical power as a function of  $\gamma$

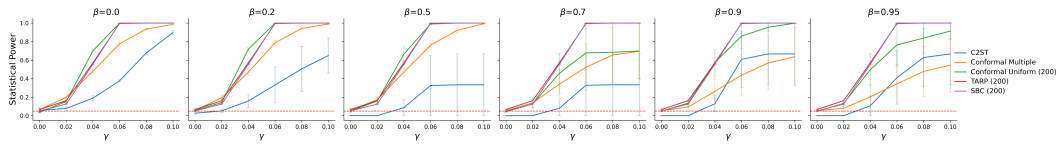


(b) Statistical power under Conformal Uniform with varying  $m$

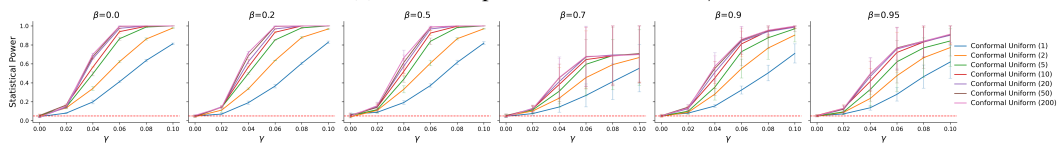


(c) Statistical Power degradation under classifier degeneration

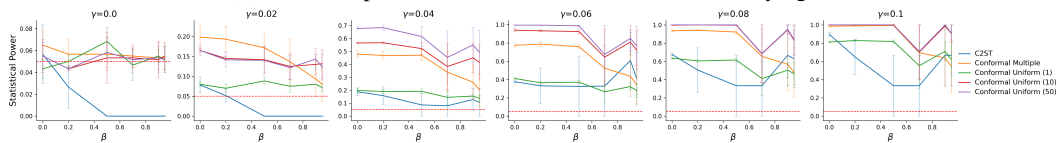
Figure 8: Power analysis under Heavy-Tailed Perturbation.



(a) Statistical power as a function of  $\gamma$

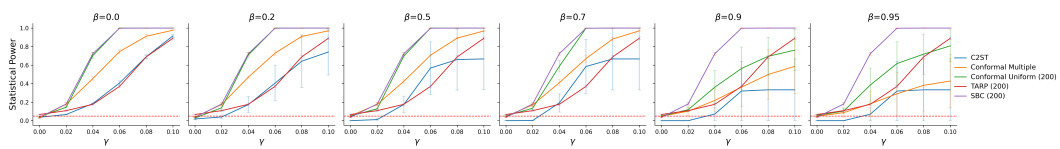


(b) Statistical power under Conformal Uniform with varying  $m$

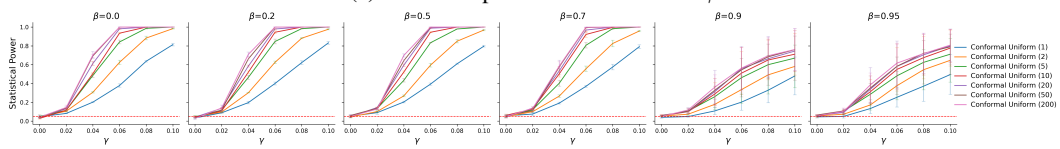


(c) Statistical Power degradation under classifier degeneration

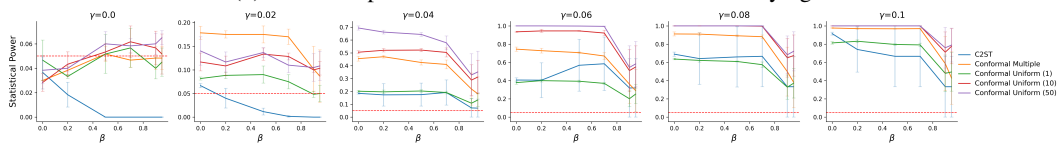
Figure 9: Power analysis under Additional Mode.



(a) Statistical power as a function of  $\gamma$



(b) Statistical power under Conformal Uniform with varying  $k$



(c) Statistical Power degradation under classifier degeneration

Figure 10: Power analysis under Mode Collapse.